FE MODEL OF A NANOPOSITIONING FLEXURE STAGE FOR DIAGNOSIS OF TRAJECTORY ERRORS

S. P. Kearney, D. Shu,
Advanced Photon Source, Argonne National Laboratory, Argonne, IL., USA

Abstract

The Advanced Photon Source Upgrade project includes upgrading several beamlines, which desire nanopositioning and fly-scan capabilities. A step towards achieving this is through the use of flexure stages with minimal trajectory errors. Typically, parasitic motion is on the order of micrometer-level displacements and tens of microradian-level rotations. The cause of such errors is difficult to diagnosis due to the scale and complexity of the overall mechanism. Therefore, an FE model of a flexure pivot nanopositioning stage with centimeter-level travel range [1, 2] has been developed to aid in trajectory error diagnosis. Previous work used an FE model and relative error analysis to quantify the effects of assembly error on trajectory errors [3]. Relative error analysis was used due to the difficulty in validating a complex FE model. This study develops an experimentally validated FE model of a single joint to quantify the expected error in the full FE model. The full model is then compared experimentally to the flexure stage to assess the model accuracy and diagnosis trajectory errors.

INTRODUCTION

The Advanced Photon Source Upgrade project includes upgrading several beamlines, which desire nanopositioning and fly-scan capabilities. This will require a better understanding the cause of trajectories that are typically on the order of micrometer displacements and mircoradian rotations [1]. We have previously developed a flexure pivot nanopositioning stage with centimeter-level travel range [1, 2] that could benefit from more focused analysis of its trajectory errors. Previously, relative error analysis was used due to the difficulty in validating a complex FE model. This study hopes to improve the quality of the FE model to be used in absolute analysis. In this paper we will present a more accurate model of the single flexure pivot that was validated through experiment, and use this more accurate model in the complete flexure stage model. The flexure stage FE model will then be compared to experimental results.

The flexure stage has four main components in its construction. A commercially available flexure pivot from C-Flex Bearing Co., Inc. and Riverhawk Co, Fig. 1, is used at each mechanical joint. These pivots are then assembled in a deformation compensated orientation four-bar mechanism, see Fig. 2. Two of these four-bar mechanisms can be joined (Fig. 3), known commonly as a double parallelogram mechanism [4], to provide rectilinear motion with the parasitic motion of the four-bar cancelled. However, there is now two degrees of freedom with the double parallelogram so we employ a 2:1 stabilizing mechanism (Fig. 4 item 2) to control the floating middle-bar, which is similar to the mechanism in [5]. A complete flexure stage, Fig. 4,

can then be assembled using these fundamental units, a vertical stage using these units can be seen in [3]. The stage in Fig. 4 will be used in this analysis.

Figure 1: Flexure pivot used as a main element in the flexure stage design.

Figure 2: Four-bar deformation compensated flexure mechanism.

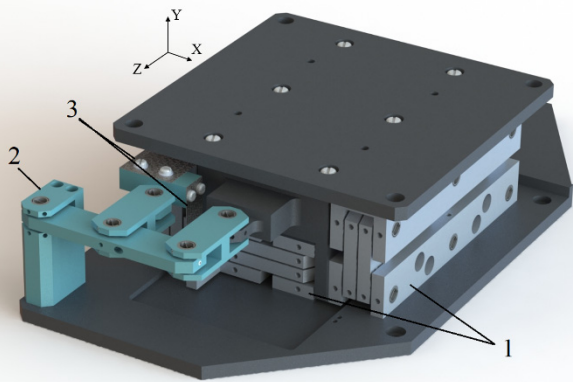Figure 3: Double four-bar deformation compensated flexure mechanism.

Figure 4: Complete model of flexure stage: (1) Double four-bar mechanisms (3 are actually used, the third is not visible on the opposite side), (2) 2:1 stabilizer mechanism, and (3) leaf flexure connections to the middle-bar. The co-ordinate frame used throughout this study is also shown.

VALIDATION OF FLEXURE PIVOT

Experimental Setup

For the FE model to more accurately predict trajectory errors, it must first accurately model the parasitic stiffness of a single flexure pivot. A setup to measure the parasitic stiffness can be seen in Fig. 5. A single flexure and link from the larger four-bar mechanism is used as the test bed. A load is applied at the end of the link, which causes the pivot to rotate about Z (using coordinate frame Fig. 4), a parasitic motion. The load is measured by a force gauge and the displacement by a 3-channel Attocube Systems AG laser interferometer (IDS3010). All 36 flexure pivots used in the stage assembly were measured and the results can be seen in Table 1. The COV for 36 flexure pivots was found to be 4%, which means that there is measurable variance in the stiffness of the pivots. The entire minimum to maximum range of stiffness varied by +8.5% and -9.2% from the mean, which agrees well with the manufacturer, C-Flex Bearing Co., Inc., rotational stiffness variance of ±10%. All of this variance in flexure pivot stiffness suggests there may be more difficulty accurately modelling the complete flexure stage.
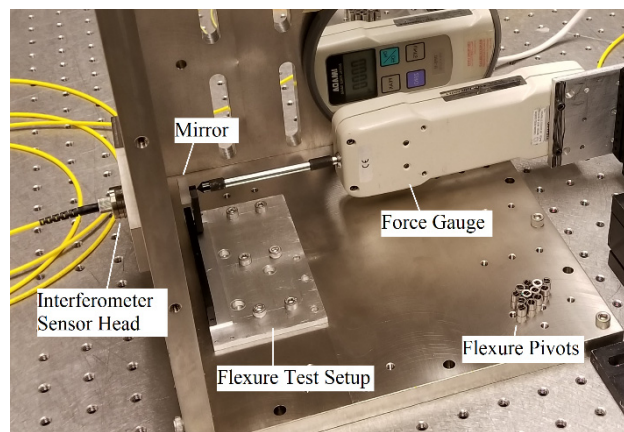

Figure 5: Experimental test setup to measure the parasitic stiffness of the flexure pivots.

FE Model Single Flexure Pivot Results

The first base FE model of the experimental setup can be seen in Fig. 6. This model was used to theoretically measure the parasitic stiffness. It can be seen that this model resembles the experiment, however this first setup, FE results row 1 in Table 1, show a 16% error. It was thought that decreasing the element size at the flexure, Fig. 7, from 0.2 mm to 0.1 mm would reduce this error, however the error was only reduced by 0.2% to 15.8%. Then the model fixture was improved to simulate the mounting screws with a no penetration but sliding and lifting virtual wall and local fixtures, Fig. 8. This also turned out to have little effect with only a 0.7% reduction in error. Finally, the bonding condition of the flexure bearing surface was redesigned to simulate the use of set screws, Fig. 9. The effect was that the error reduced to -2.4%, which is within the COV of the experimental setup. This final model was then used to find the smallest number of mesh elements and type of mesh that would keep the same accuracy. It was found that a curvature based mesh with 0.25 mm elements for the flexures, 0.65 mm elements for the simulated set screws, and that removal of the flexure side rounds was the optimal mesh, see Fig. 10.
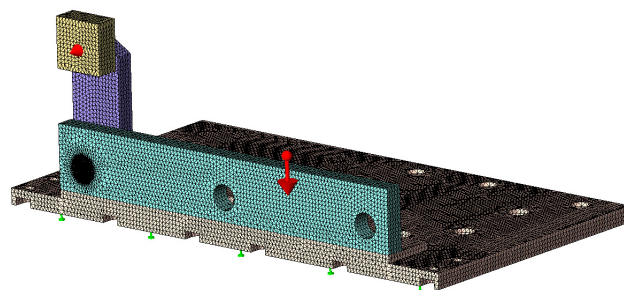

Figure 6: FE model of single flexure pivot setup. The green arrows represent fixtures, red arrow in center is the gravity force, and red arrow protruding from the mirror if the force direction and measurement point.
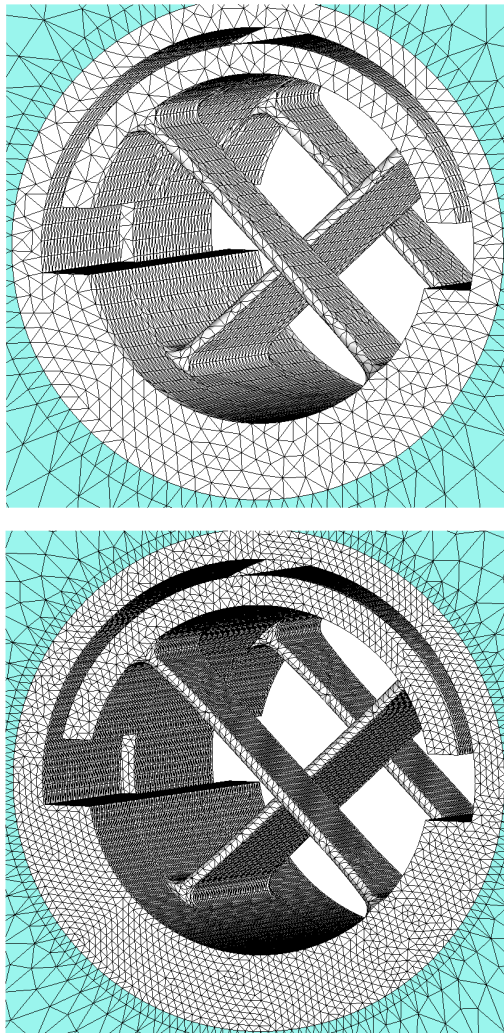
Figure 7: Varying mesh element size: top element size is 0.2 mm and bottom element size is 0.1 mm.
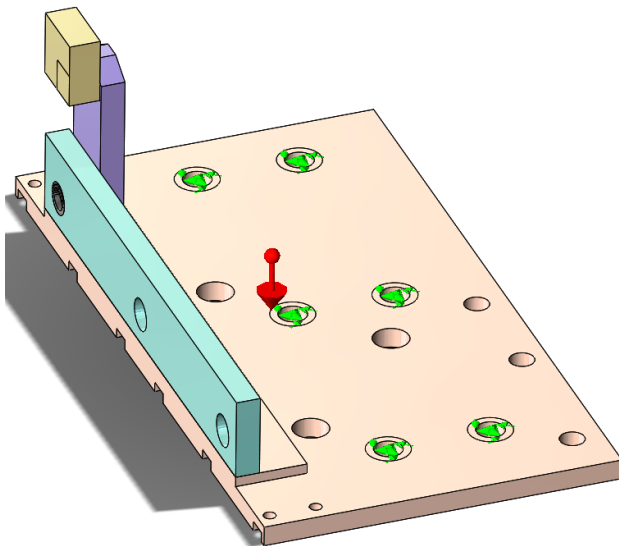

Figure 8: Base fixture now simulated by virtual wall with no penetration and simulated bolt fixtures.
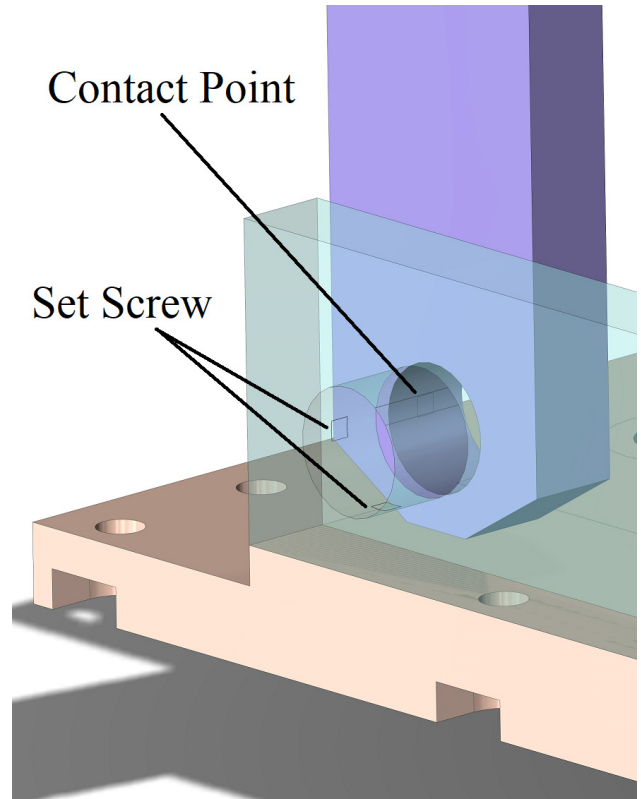

Figure 9: FE model using simulated set screw contact instead of bonded contact for the entire pivot bearing face.
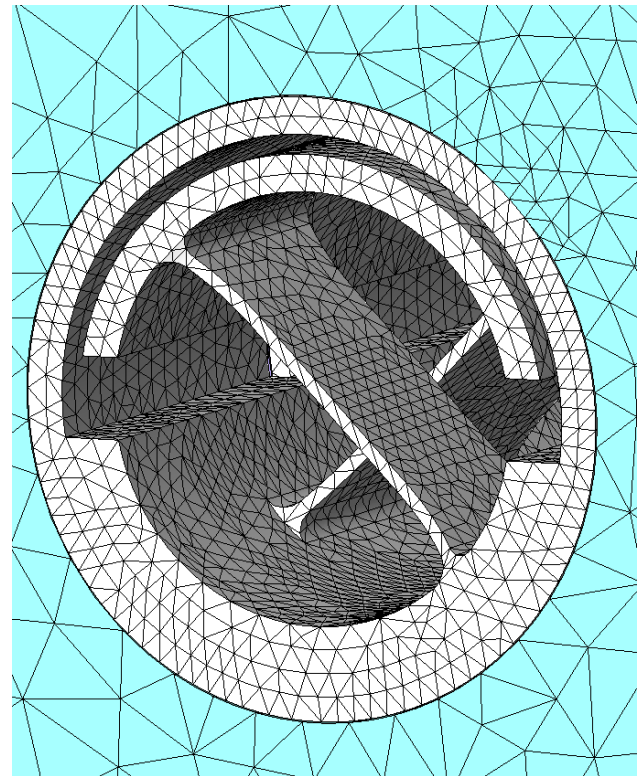

Figure 10: Optimized curvature based mesh with fillet features on the flexure sides removed. The fillets at the weld points of the flexure are retained.

Table 1: Experimental and FEA Results. K, is the parasitic stiffness of the flexure pivot, 36 pivots were measured, σ is the standard deviation, and COV is the coefficient of variation. Each row in the FEA results represents a different FE model

Experiment Results	K (N/µm)	σ	COV
Flexure Pivots	0.0317	0.0013	4.0 %
FEA Results	**K (N/µm)**	**Error**	
1. 0.2 mm Elements	0.0368	16.0 %	
2. 0.1 mm Elements	0.0367	15.8 %	
3. Base Fixture Complex Simulation	0.0365	15.3 %	
4. Set Screws Simulated	0.0309	-2.42 %	

Figure 11: Experimental setup of the complete flexure stage. The mirror on the left was used to measures displacement and a flat rectangular mirror on the right to measure pitch and roll.

COMPLETE FE MODEL COMPARED TO EXPERIMENT

A larger complete FE model using the refined model from the single flexure pivot experiment was then compared to experiment using the complete flexure stage. Figure 11 shows the experimental setup of the flexure stage. It was driven using a Newport Co. PZA12 piezo actuator over a range of ±3 mm. The same interferometer was used to measure the stage displacement and pitch about the Z axis. It was clamp-mounted to an Invar frame at three points that were simulated in the FE model. The FE model can be seen in Fig. 12. The orientation of the flexure pivots was matched between the FE model and the actual stage. The entire model had approximately 4.5×10^6 elements and used the large displacement method, which applies a percent of the load in each step and updates the model deformation before moving on to the next step. Each solution point took from 30 min – 1.5 hours depending on the size of the displacement step.

A comparison of the FEA data to the measured experimental data of 3 runs can be seen in Fig. 13. Each individual run is offset from the previous due to thermal drifting variances in the mounting interface between the mirror and the moving plate of the stage. It can be seen that the FE model does not agree with the experimental results. The trend of the FEA data does go in the same direction as the experimental data, so there may be some parts of the model that are working. However, the model and experiment are so far off that there must be some major mechanical bending, assembly error, or manufacturing tolerance that is not being modelled. This is especially evident by the approximate first order linearity of the FEA data, which does not match the exponential pitch curve of the experiment.
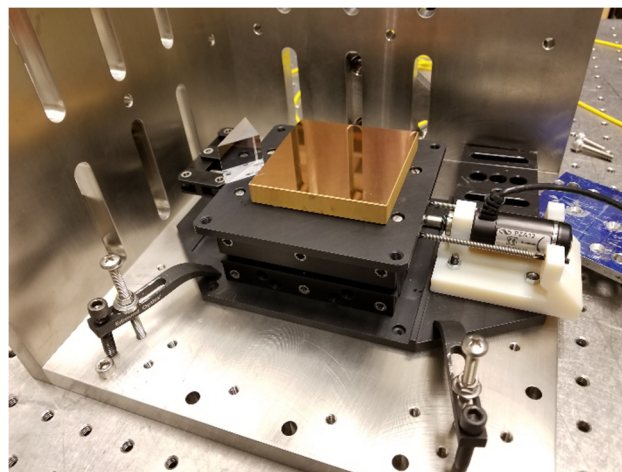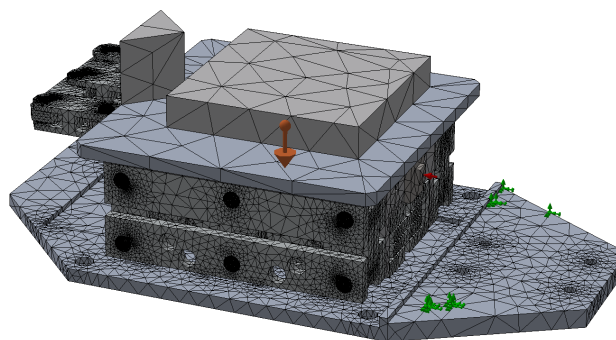

Figure 12: FE model of complete flexure stage. The orange arrow in the center is the gravity force, the red arrow an applied displacement, and the green arrows the fixed points.
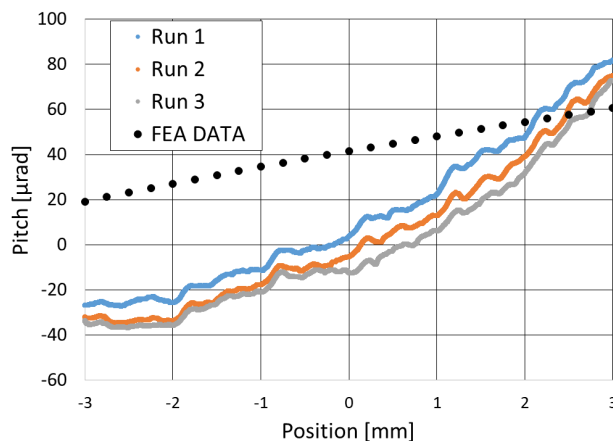

Figure 13: Pitch trajectory errors (about X) for three experimental runs in the same direction compared to the FEA results.

CONCLUSION

The parasitic stiffness of 36 flexure pivots was experimentally measured in order to validate an FE model of a single flexure pivot. The FE model of a single flexure pivot was found to be accurate to an experimentally measured flexure pivot with -2.4% error. In order to achieve this accuracy it was found that it is crucial to include an accurate simulation of the mounting method used for the flexure pivot. In addition, the entire range of flexure pivot stiffness was found to be 8.5% to -9.2% from the mean, which means that this tolerance may need to be incorporated into future FE models.

The FE model of a single flexure pivot was then used in a larger FE model of a flexure pivot stage. It was expected that with the more accurate single unit the larger FE model would predict the trajectory errors of the actual flexure pivot stage. However, it was found that this was not the case. The FE model was unable to predict the trajectory errors of the flexure stage. This result suggests that many physical features have yet to be accurately modelled in this complex FE model such that it is not yet ready for absolute prediction. Future work into this model will need to incorporate the following features:

- Geometric tolerance from manufacturing
- Set screw holding torque
- Set screw tightening order
- Assembly errors
- Flexure pivot stiffness variance
- All components interfaces (bonded vs. simulated bolt fixture)

Previous work in [3] used a large and complex FE model with relative analysis to identify design features that were sensitive to misalignment. Such relative analyses will be useful in identifying key features of the above list. By identifying which features must be modelled and which are not as sensitive we can keep the complete FE model to a practical level of complexity in regards to computing capability. A better understanding how these features affect the model as compared to the actual stage will provide more than just better FE models, but will contribute to better design insight that will aid in the design of future nanopositioning flexure stages.

REFERENCES

[1] D. Shu *et al.*, "Design and test of precision vertical and horizontal linear nanopositioning flexure stages with centimeter-level travel range for x-ray instrumentation", in *Proc. SPIE*, vol. 10371, 2017.

[2] U.S. Patent granted No. 8,957,567, D. Shu, S. Kearney, and C. Preissner, 2015.

[3] S. Kearney, D. Shu., "Trajectory error analysis of a flexure pivot type guide for linear nanopositioning", In *Proc. SPIE*, vol. 10371, 2017.

[4] S. T. Smith, *Flexures: elements of elastic mechanisms*, CRC Press; 2000.

[5] R. M. Panas, "Large displacement behavior of double parallelogram flexure mechanisms with underconstraint eliminators", in *Precision Engineering*, 46, 2016, pp. 399-408.